

Static and harmonic analysis of moderately thick square sandwich plate using FEM

Manoj Nawariya*¹, Avadesh K. Sharma², Pankaj Sonia³ and Vijay Verma⁴

¹Department of Mechanical Engineering, IPS College of Technology and Management, Gwalior, 474001 India

²Department of Mechanical Engineering, Rajkiya Engineering College, Mainpuri, 205119, India

³Department of Mechanical Engineering, GLA University, Mathura, UP, 281406, India

⁴Department of Mechanical Engineering, Bundelkhand Institute of Engineering & Technology, Jhansi, 284128, India

(Received January 3, 2021, Revised December 10, 2021, Accepted September 25, 2022)

Abstract. In this paper, sandwich plate, constructed with orthotropic and isotropic composite materials, is analyzed to obtain the static and harmonic behavior. The analysis is done by using ANSYS APDL FEM tool. A solid-shell 190 and an 8-node solid 185 elements are employed for face and core material respectively to analyze the plate. Results was attained by using Reissner-Mindlin theory. Effect of increasing thickness ratio of face sheet to depth of the plate is presented on static, vibration and harmonic response on the sheet and the results are discussed briefly. Published work in open domain was used to validate the results and observed excellent agreement. It can be stated that proposed model presents results with remarkable accuracy. Results are obtained to reduce the weight of the plate and minimizing the vibration amplitudes.

Keywords: ANSYS; FEM; Harmonic analysis; sandwich plate; static analysis

1. Introduction

In the modern era, conventional composite plates are replaced by sandwich plates. Sandwich structures are manufactured by two face sheet above and below supported with a core of different material. Both sheets are glued to core material with a particular adhesive. Sandwich structure is one of the most successful areas of research and development in composite materials field. For this reason, much research work has been devoted in the field of sandwich structure. Static and vibration response of sandwich structure have been studied by many researchers.

Hanna and Leissa (1994) for vibration of thick plate proposed a Reissner-Mindlin theory for higher order. Free vibration analysis of sandwich structure was studied by using HSDT and p -Ritz technique. Effect of material property, thickness of plate, boundary condition etc has been analysed (Meunier and Shenoit 1999, Wang *et al.* 2000). Caprino *et al.* (1999) carried out experiments on epoxy reinforced with woven carbon shields of varying thicknesses. At initiation point author determine the strength and energy, the peak strength, corresponding energy and infiltration energy.

*Corresponding author, Ph.D., E-mail: drmanoj.academic@gmail.com

For dynamic investigation of composite and sandwich plate, new element was developed by Kulkarni and Kapuria (2008). Author found that the new developed division, founded on III-order zigzag concept, is suitable for normal finite element programming.

Icardi and Ferrero (2009) presented impact analysis on sandwich composites using FEM technique based on a refined plate element with strain energy updating process. Malekzadeh and sayyidmousavi (2009) considered vibration examination of quadrilateral sandwich sheet with elastic core using FEM technique through APDL. Authors obtained the result for various parameters and found that involved mass decrease frequency of sandwich sheet. Abdennadher *et al.* (2009) developed a mathematical model to study dynamic response of the viscoelastic sandwiches plates in the presence of shock. Shariyat (2010) analysed bending and vibration behaviour of sandwich sheet exposed to combine thermal and mechanical load through introducing generalized global-local concept. A new optimal result is developed aimed at analysis of sandwich structure used to solve the problems of flexural as well as torsion at the least weight (Li *et al.* 2011). Author identified three design cases and also derived their pertinent optimum solutions. Gopichand *et al.* (2012) made a sandwich panel with mild steel as a core and stainless steel as a face sheet. They obtained the simulation result of compressive strength using ANSYS Workbench and compared these result with experimental data. Authors observed the maximum stress at the top surface of sandwich panel. Abo Sabah and Kueh (2014) examined the effects of interface element on the behaviour of a two-layer composite plate in the presence of impact load employing zero-thickness interface element by using finite element method. Lashin and El-Nady (2015) analyzed the sandwich beam for calculating the natural frequencies and mode shapes under different boundary conditions. Mondal *et al.* (2015) analyzed the sandwich plates with cut outs at different locations and determined the effects of thickness of core and face sheet, cut out diameter etc. on frequencies of various modes. Krzyzak *et al.* (2016) studied the Sandwich Structured Composites used in Aeronautics and found that manufacturing method to construct the sandwich component shows the significant effect on mechanical properties. Soufeiani *et al.* (2017) studied the dynamic analysis of laminated FRP slab for different stacking sequences subjected to human-induced loads using FE techniques. Belarbi *et al.* (2017) developed a layerwise FE model for the static analysis of sandwich plates and laminated composite to study vibrational behavior. Rezaiee-Pajand *et al.* (2018) presented the stretching effects on shell thickness considering seven-parameter triangular element. Pagani *et al.* (2018) analyzed static behaviour sandwich as well as composite plates using 2D MITC finite element. They tested the plate element by comparing the different theories of finite element. Rezaiee-Pajand *et al.* (2018) investigated static characteristics of non-prismatic sandwich FG beams applying principle of minimum total potential energy. Rezaiee-Pajand *et al.* (2018) analyzed a buckling and free vibration behavior of tapered FGM sandwich column. Rezaiee-Pajand *et al.* (2019) perform nonlinear investigation of FG-sandwich sheets and thin vessel using ESL theory. Author uses CNT infused composite laminate with in-plane piling to analyze nonlinear static and vibration response by using six-node triangular element. Al-Fasih *et al.* (2020) investigated practically and mathematically using four point loading scheme the quasi static fracture performance of sandwich honeycomb composite beams encompassing crack at the skin. From the literature survey, it has come to know that static and shaking examination of different sheets have performed by several researchers using different techniques. Harmonic analysis of sandwich plate not reported in the literatures presented in this article.

2. Modeling

Table 1 Thickness of sandwich plates of 6-geometries (Kulkarni *et al.* 2008)

Geometry No.	Proportion of height of the sheet to depth of the plate (T/h)		
	For top face sheet (T_1/h) of each ply	For core material (T_c/h)	For bottom face sheet (T_2/h) of each ply
1	0	1.0	0
2	0.04/0.04 [for 0°/90° cross ply]	0.84	0.04/0.04 [for 90°/0° cross ply]
3	0.05/0.05 [for 0°/90° cross ply]	0.80	0.05/0.05 [for 90°/0° cross ply]
4	0.07/0.07 [for 0°/90° cross ply]	0.72	0.07/0.07 [for 90°/0° cross ply]
5	0.09/0.09 [for 0°/90° cross ply]	0.64	0.09/0.09 [for 90°/0° cross ply]
6	0.11/0.11 [for 0°/90° cross ply]	0.56	0.11/0.11 [for 90°/0° cross ply]

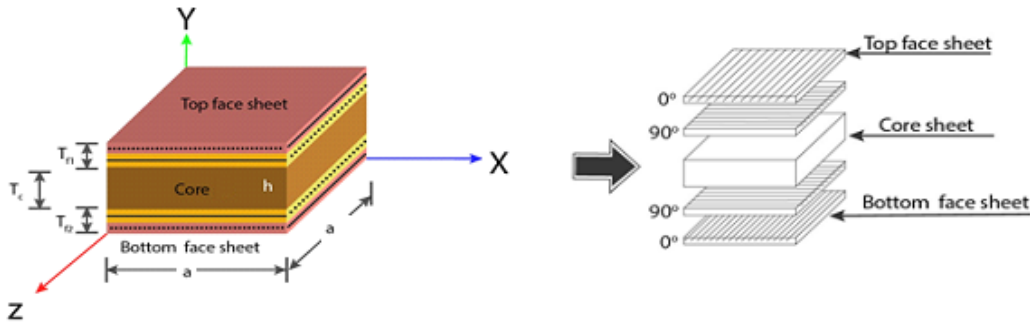


Fig. 1 Representation of piling sequence and final representation of sandwich sheet

2.1 Geometric modeling

Six sandwich plates of different geometries (shown in Table 1) with (0°/90°/Core/90°/0°) piling arrangement are taken to analyze the result. Fig. 1 presents the geometry of the plate.

Height of upper and lowest face plate are varied from “0h” to “0.22h” and thickness of core material is varied from “1h” to “0.56h”.

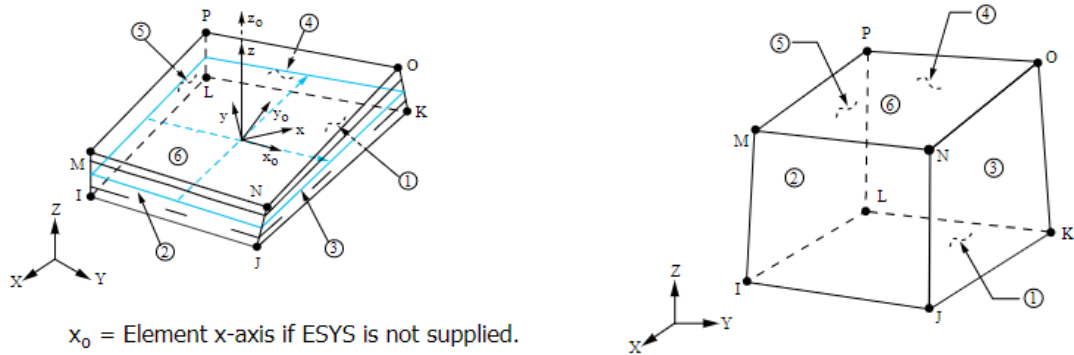
Where ‘h’ is the depth of plate taken as unity and side of square block is “a”.

2.2 FE modeling

A solid-shell 190 element is considered for face sheet and an 8-node solid 185 is considered to mesh central material as shown in Fig. 2 (a) and (b). SOLID185 section is appropriate to model all-purpose 3-D solid assemblies. It permits prism, tetrahedral, and pyramid degenerations for uneven areas. SOLSH190 is utilized for simulating variable thickness hollow construction.

2.3 Boundary condition

The boundary condition applied on the sandwich plate is shown in Table 2 and Fig. 3.



x_0 = Element x-axis if ESYS is not supplied.
 x = Element x-axis if ESYS is supplied.

(a) SOLSH190 element for face sheet

(b) 8-node solid 185 to mesh central material

Fig. 2 FE modeling elements

Table 2 Boundary condition applied on the square sandwich plate

Analysis Type	Boundary Condition (BC)	Force (F)
Static Analysis	Fixed all edges (CCCC)	1000 N in vertical direction at every node of top face sheet
Vibration Analysis	Fixed all edges (CCCC)
Harmonic Analysis	Fixed all edges (CCCC)	1000 N in vertical direction at every node of top face sheet

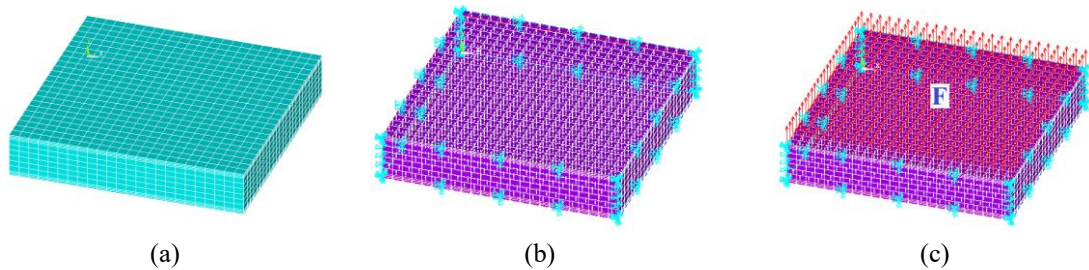


Fig. 3 (a) Meshed geometry of plate (b) Plate with clamped BC (c) Clamped plate with force of 1000 N

2.4 Material property

Square sandwich plate is made of two types of materials i.e., orthotropic and isotropic. In this study, orthotropic Material is taken for face sheet and Isotropic material is taken for core. Properties of both materials were tabulated in Table 3.

3. Mathematical formulation

Reissner-Mindlin theory is adopted to examine the sheet. This theory provides a bridge between correctness and computational competence for determining structural behaviour of plates.

3.1 Strain displacement relations

Table 3 Materials property

Property	Face sheet Material (1)	Core Material (2)	Reference
Young's Modulus in X direction	276 GPa	0.5776 GPa	
Young's Modulus in Y direction	6.9 GPa	0.5776 GPa	
Young's Modulus in Z direction	6.9 GPa	0.5776 GPa	
Shear Modulus for surface (xy) of the plate	6.9 GPa	0.1079 GPa	
Shear Modulus for surface (yz) of the plate	6.9 GPa	0.22215 GPa	Kulkarni <i>et al.</i>
Shear Modulus for surface (xz) of the plate	6.9 GPa	0.1079 GPa	(2008)
Poisson's Ratio for surface (xy) of the plate	0.25	0.0025	
Poisson's Ratio for surface (yz) of the plate	0.25	0.0025	
Poisson's Ratio for surface (xz) of the plate	0.3	0.0025	
Density	681.8 kg/m ³	1000 kg/m ³	

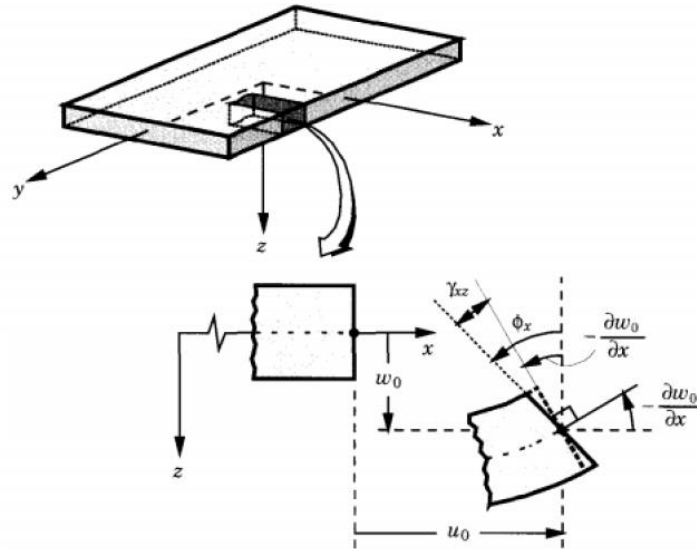


Fig. 4 Deformed & undeformed shape (Reddy 1997)

Displacement fields are articulated as (Reddy 1997)

$$\left. \begin{aligned} u(x, y, z, t) &= u_0(x, y, t) + z\phi_x(x, y, t) \\ v(x, y, z, t) &= v_0(x, y, t) + z\phi_y(x, y, t) \\ w(x, y, z, t) &= w_0(x, y, t) \end{aligned} \right\} \quad (1)$$

Where (u_0, v_0, w_0) shows translations at $(z=0)$ plane; Note that

$$\frac{\partial u}{\partial z} = \phi_x \text{ (revolution of transverse normal to y-axes)} \quad (2)$$

$$\frac{\partial v}{\partial z} = \phi_y \text{ (revolution of transverse normal to x-axes)} \quad (3)$$

Fig. 4 shows displacement and stresses before and after deformation on periphery of the plate under the assumptions of FSDT.

The followings are the expression of strain displacement relations.

Along middle surface, in-plane strains were

$$\epsilon_x^0 = \frac{\partial u_0}{\partial x} \quad (4)$$

$$\epsilon_y^0 = \frac{\partial v_0}{\partial y} \quad (5)$$

$$\epsilon_{xy}^0 = \frac{\partial u_0}{\partial y} + \frac{\partial v_0}{\partial x} \quad (6)$$

The arches are

$$K_x^0 = \frac{\partial \phi_x}{\partial x} \quad (7)$$

$$K_y^0 = \frac{\partial \phi_y}{\partial y} \quad (8)$$

$$K_{xy}^0 = \frac{\partial \phi_x}{\partial y} + \frac{\partial \phi_y}{\partial x} \quad (9)$$

The shear strains along xz and yz surfaces are

$$\epsilon_{xz} = \phi_x + \frac{\partial w_0}{\partial x} \quad (10)$$

$$\epsilon_{yz} = \phi_y + \frac{\partial w_0}{\partial y} \quad (11)$$

The strain constituent at a point is

$$\begin{Bmatrix} \epsilon_{xx} \\ \epsilon_{yy} \\ \epsilon_{yz} \\ \epsilon_{xz} \\ \epsilon_{xy} \end{Bmatrix} = \begin{Bmatrix} \epsilon_{xx}^{(0)} \\ \epsilon_{yy}^{(0)} \\ \epsilon_{yz}^{(0)} \\ \epsilon_{xz}^{(0)} \\ \epsilon_{xy}^{(0)} \end{Bmatrix} + z \begin{Bmatrix} K_{xx}^{(0)} \\ K_{yy}^{(0)} \\ 0 \\ 0 \\ K_{xy}^{(0)} \end{Bmatrix} \quad (12)$$

$$\begin{Bmatrix} \epsilon_{xx} \\ \epsilon_{yy} \\ \epsilon_{yz} \\ \epsilon_{xz} \\ \epsilon_{xy} \end{Bmatrix} = \begin{Bmatrix} \frac{\partial u_0}{\partial x} \\ \frac{\partial v_0}{\partial y} \\ \phi_y + \frac{\partial w_0}{\partial y} \\ \phi_x + \frac{\partial w_0}{\partial x} \\ \frac{\partial u_0}{\partial y} + \frac{\partial v_0}{\partial x} \end{Bmatrix} + z \begin{Bmatrix} \frac{\partial \phi_x}{\partial x} \\ \frac{\partial \phi_y}{\partial y} \\ 0 \\ 0 \\ \frac{\partial \phi_x}{\partial y} + \frac{\partial \phi_y}{\partial x} \end{Bmatrix} \quad (13)$$

3.2 Constitutive equations

For orthotropic lamina association of stress-strain are as follows (Reddy 1997)

$$\begin{Bmatrix} \sigma_{xx} \\ \sigma_{yy} \\ \sigma_{xy} \end{Bmatrix}^{(k)} = \begin{bmatrix} \bar{Q}_{11} & \bar{Q}_{12} & \bar{Q}_{16} \\ \bar{Q}_{12} & \bar{Q}_{22} & \bar{Q}_{26} \\ \bar{Q}_{16} & \bar{Q}_{26} & \bar{Q}_{66} \end{bmatrix}^{(k)} \begin{Bmatrix} \varepsilon_{xx} \\ \varepsilon_{yy} \\ \varepsilon_{xy} \end{Bmatrix} \quad (14)$$

$$\begin{Bmatrix} \sigma_{yz} \\ \sigma_{xz} \end{Bmatrix}^{(k)} = \begin{bmatrix} \bar{Q}_{44} & \bar{Q}_{45} \\ \bar{Q}_{45} & \bar{Q}_{55} \end{bmatrix}^{(k)} \begin{Bmatrix} \varepsilon_{yz} \\ \varepsilon_{xz} \end{Bmatrix} \quad (15)$$

where

$$\begin{aligned} \bar{Q}_{11} &= Q_{11} \cos^4 \theta + 2(Q_{12} + 2Q_{66}) \sin^2 \theta \cos^2 \theta + Q_{22} \sin^4 \theta \\ \bar{Q}_{12} &= (Q_{11} + Q_{22} - 4Q_{66}) \sin^2 \theta \cos^2 \theta + Q_{12} (\sin^4 \theta + \cos^4 \theta) \\ \bar{Q}_{22} &= Q_{11} \cos^4 \theta + 2(Q_{12} + 2Q_{66}) \sin^2 \theta \cos^2 \theta + Q_{22} \sin^4 \theta \\ \bar{Q}_{16} &= (Q_{11} - Q_{12} - 2Q_{66}) \sin \theta \cos^3 \theta + (Q_{12} - Q_{22} + 2Q_{66}) \sin^3 \theta + \cos \theta \\ \bar{Q}_{26} &= (Q_{11} - Q_{12} - 2Q_{66}) \sin^3 \theta \cos \theta + (Q_{12} - Q_{22} + 2Q_{66}) \sin \theta + \cos^3 \theta \\ \bar{Q}_{66} &= (Q_{11} + Q_{22} - 2Q_{12} - 2Q_{66}) \sin^2 \theta \cos^2 \theta + Q_{66} (\sin^4 \theta + \cos^4 \theta) \\ \bar{Q}_{44} &= Q_{44} \cos^2 \theta + Q_{55} \sin^2 \theta \\ \bar{Q}_{45} &= (Q_{55} - Q_{44}) \cos \theta \sin \theta \\ \bar{Q}_{55} &= Q_{44} \sin^2 \theta + Q_{55} \cos^2 \theta \end{aligned} \quad (16)$$

The stiffness constants $Q_{ij}^{(k)}$ for the k^{th} layer are

$$\begin{aligned} Q_{11}^{(k)} &= \left[\frac{E_x^{(k)}}{1 - \nu_{xy}^{(k)} \left(\frac{E_y^k}{E_x^{(k)}} \right)} \right], \quad Q_{22}^{(k)} = \left[\frac{E_y^{(k)}}{1 - \nu_{xy}^{(k)} \left(\frac{E_x^k}{E_y^{(k)}} \right)} \right], \\ Q_{12}^{(k)} &= \left[\frac{\nu_{xy}^{(k)} E_y^{(k)}}{1 - \nu_{xy}^{(k)} \left(\frac{E_x^k}{E_y^{(k)}} \right)} \right] \end{aligned} \quad (17)$$

Orthotropic layered composite sheet having symmetric and anti-symmetric cross-ply we have

$$Q_{66}^{(k)} = G_{xy}^{(k)}, Q_{16}^{(k)} = Q_{26}^{(k)} = 0, A_{16} = A_{26} = 0, B_{16} = B_{26} = 0, D_{16} = D_{26} = 0 \quad (18)$$

$$Q_{44}^{(k)} = G_{yz}^{(k)}, Q_{55}^{(k)} = G_{zx}^{(k)}, Q_{45}^{(k)} = 0, A_{45} = 0 \quad (19)$$

3.3 Equations of motion

Hamilton's principle were utilized for forming the equation of motion: (Reddy 1997)

$$0 = \int_0^T (\delta U + \delta V - \delta K) dt \quad (20)$$

This gives the virtual straining and kinematic energy, and work done, by the applied forces. With illimitable coordinates and stress resultants, we have motion equation as (Reddy 1997)

$$\frac{\partial N_x}{\partial x} + \frac{\partial N_{xy}}{\partial y} = \alpha_{uv} \left(I_0 \frac{d^2 u}{dt^2} + I_1 \frac{d^2 \phi_x}{dt^2} \right) \quad (21)$$

$$\frac{\partial N_{xy}}{\partial x} + \frac{\partial N_y}{\partial y} = \alpha_{uv} \left(I_0 \frac{d^2 u}{dt^2} + I_1 \frac{d^2 \phi_y}{dt^2} \right) \quad (22)$$

$$\frac{\partial Q_x}{\partial x} + \frac{\partial Q_y}{\partial y} + q(t) = I_0 \frac{d^2 w}{dt^2} \quad (23)$$

$$\frac{\partial M_x}{\partial x} + \frac{\partial M_{xy}}{\partial y} - Q_z = I_1 \frac{d^2 u}{dt^2} + I_1 \frac{d^2 \phi_x}{dt^2} \quad (24)$$

$$\frac{\partial M_{xy}}{\partial x} + \frac{\partial M_y}{\partial y} - Q_y = I_1 \frac{d^2 v}{dt^2} + I_1 \frac{d^2 \phi_y}{dt^2} \quad (25)$$

The inertias are defined as follows

$$(I_0, I_1, I_2) = \sum_{k=1}^n \int_{z_k}^{z_{k+1}} \rho^{(k)}(1, z, z^2) dz \quad (26)$$

4. Result and discussion

A quadrangular sandwich sheet is analysed to obtain results of vibration and harmonic responses. The static analysis is also conducted to check the strength of the various geometries of the plate.

The non-dimensionalized frequencies for square plate with $R=a/h$ are as follows:

For plate geometry 1: Non-dimensionalized fundamental frequency [$\varpi = \omega_n(aR/\pi^2)\sqrt{(\rho_c/Y_c)}$]

For plate geometry 2,3,4,5,6: Non-dimensionalized fundamental frequency [$\varpi = 100\omega_n a\sqrt{(\rho_c/Y_{f1})}$]

It has been observed that the reduction in weight of sandwich plate occurs through enhancing thickness of face plate as shown in Fig. 6 and T able 4.

The convergence behaviour has been verified and found converged frequency at (24×24) mesh size. It can be said that this mesh size is sufficient to get the responses. In addition, the responses obtained have also been compared with the available publication to validate the results.

4.1 Convergence study

Non-dimensionalised frequencies upto six modes have been computed to find the proper mesh size considering R (side to depth ratio) as 10. The converged frequencies have been found at mesh

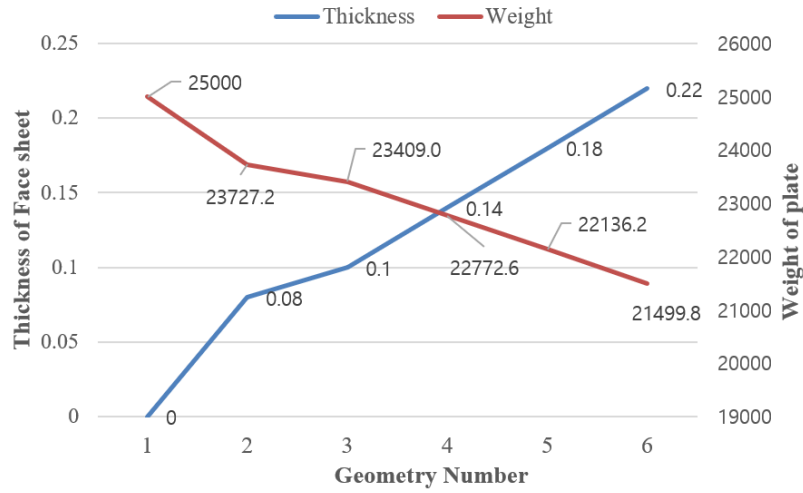


Fig. 5 Variation of face plate thickness with inertia of sheet

Table 4 Proportion reductions in the inertia of sheet of different geometries with various thicknesses and $h=1$ depth of sheet

Specimen No.	Proportion of thickness with depth of sheet (T/h)			Inertia of Sheet (N)	% Decrease in Inertia
	For top face sheet (T_t/h)	For core material (T_c/h)	For bottom face sheet (T_b/h)		
1	0	1.0	0	25000	0
2	0.08	0.84	0.08	23727.2	5.09
3	1.10	0.80	1.10	23409.0	6.36
4	0.14	0.72	0.14	22772.6	8.91
5	0.18	0.64	0.18	22136.2	11.46
6	0.22	0.56	0.22	21499.8	14.00

Table 5 Non-dimensionalized frequencies upto 6 mode for a square sandwich plate under CCCC

Mode No.	Non-dimensionalized fundamental frequency (ω)							
	M × N							
	12×12	16×16	18×18	20×20	22×22	24×24	26×26	28×28
M ₁	9.6290	9.5032	9.4836	9.4696	9.4586	9.4507	9.4450	9.4405
M ₂	16.1490	15.7676	15.7317	15.7045	15.6829	15.6656	15.6508	15.6383
M ₃	16.5024	16.2299	16.1868	16.1558	16.1328	16.1154	16.1018	16.0912
M ₄	21.4854	21.0212	20.9623	20.9203	20.8889	20.8643	20.8447	20.8284
M ₅	25.0795	24.4328	24.2702	24.1519	24.0631	23.9954	23.9425	23.9005
M ₆	25.3978	24.6486	24.5023	24.4006	24.3266	24.2710	24.2283	24.1946

size of (24×24) as shown in Table 5.

4.2 Comparison study

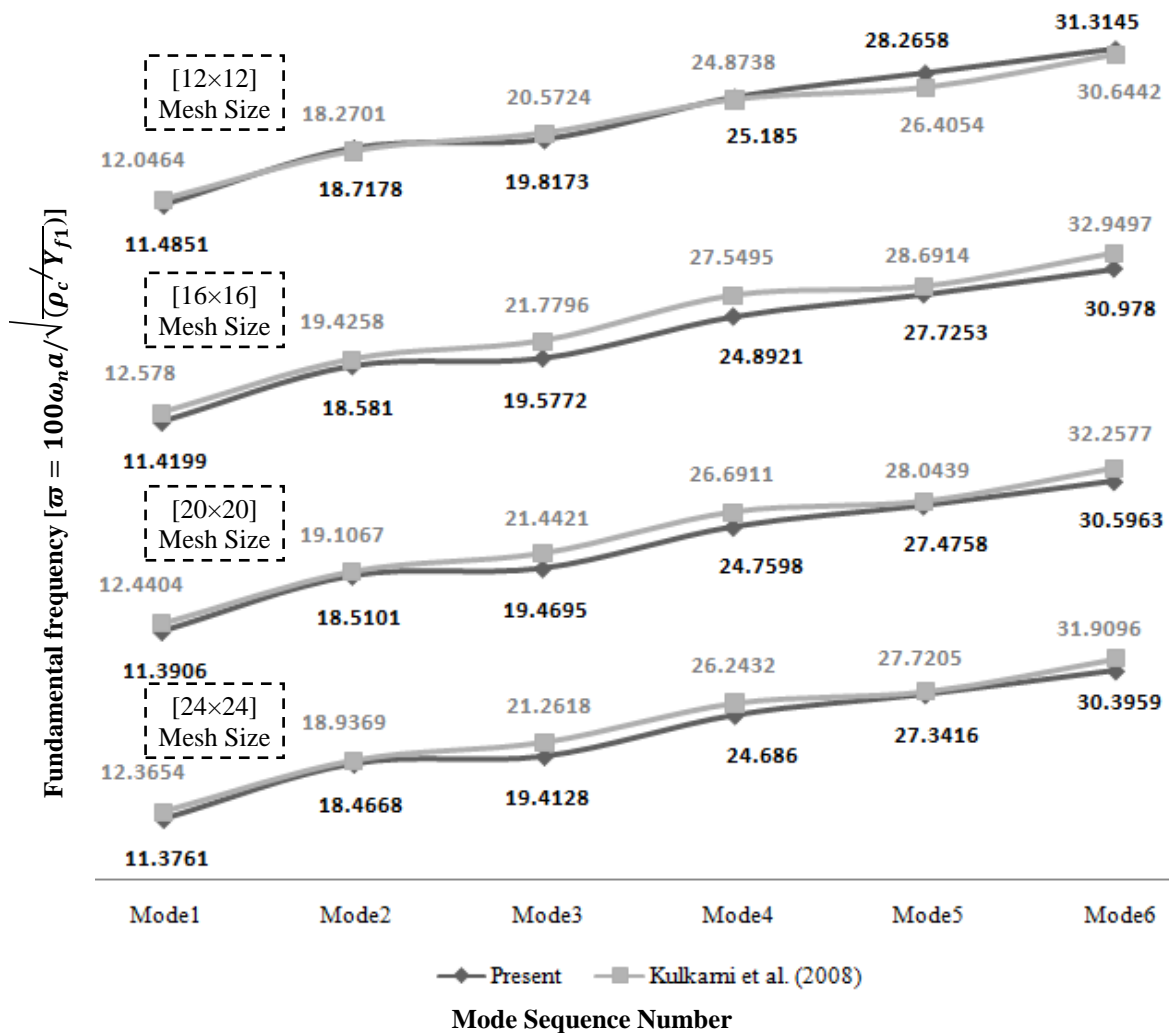


Fig. 6 Comparison of frequencies parameter for different Mesh Size

To validate the present result, Frequency parameters ($\bar{\omega}$) have been compared with literature of Kulkarni *et al.* (2008). The clamped sandwich plate with $(0^\circ/90^\circ/\text{Core}/90^\circ/0^\circ)$ lamination scheme has been taken to compare for various mesh sizes taking R as 5. The comparison is shown in Fig. 6 and it is found that results are much similar.

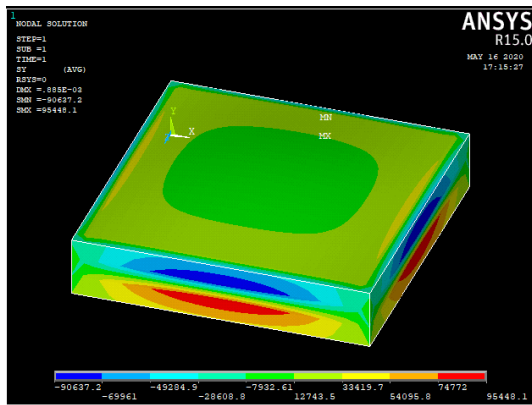
4.3 Static analysis

Table 6 presents maximum stresses in the vertical direction and percentage decrease in stress with varying faceplate thickness. It has been observed that when no face sheet is added to construct a plate, the stress is high. Thus by introducing a very thin faceplate (thickness-0.8h), stress decreases by 74.35%. Increasing faceplate thickness will further decrease the stress.

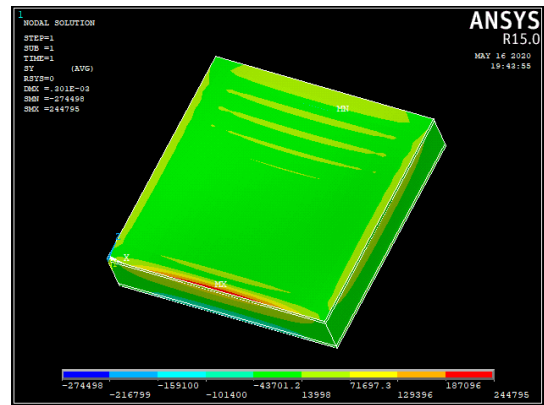
Fig. 7 (a)-(f) present the nodal solution of stress for different geometry of plates.

Table 6 Maximum stresses in vertical direction and % reduction in stresses for increasing thickness of face sheet

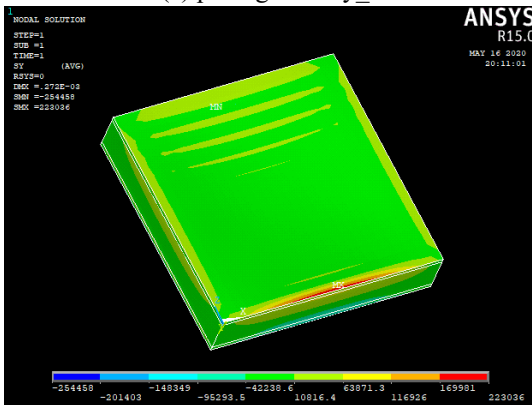
Geometry No.	Ratio of thickness of the faceplate to depth of plate			Maximum Stress (N/m ²)	% reduction in stress
	For top face sheet (T_1/h)	For core material (T_c/h)	For bottom face sheet (T_2/h)		
1	0	1.0	0	9.54460×10^5	0.00
2	0.08	0.84	0.08	2.44790×10^5	74.35
3	0.10	0.80	0.10	2.22026×10^5	76.74
4	0.14	0.72	0.14	1.80074×10^5	81.13
5	0.18	0.64	0.18	1.41609×10^5	85.16
6	0.22	0.56	0.22	1.11462×10^5	88.32



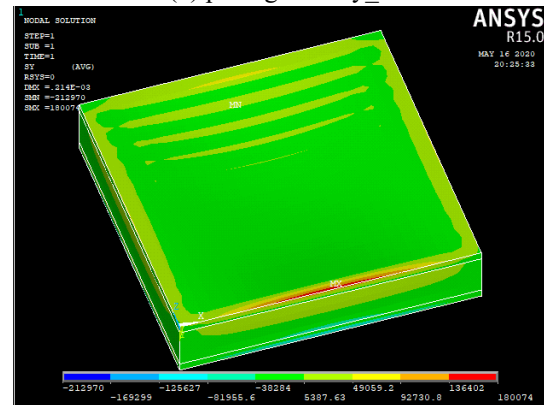
(a) plate geometry_1



(b) plate geometry_2



(c) plate geometry_3



(d) plate geometry_4

Fig. 7 Nodal Solution for various plate geometry

4.4 Vibration analysis

In present study, ten modes of frequency have been determined for square sandwich plate to observe effects of increasing thickness proportion of face sheets with depth of sheet on frequency parameters. The 24×24 mesh size and clamped boundary conditions of all edges of the plate has

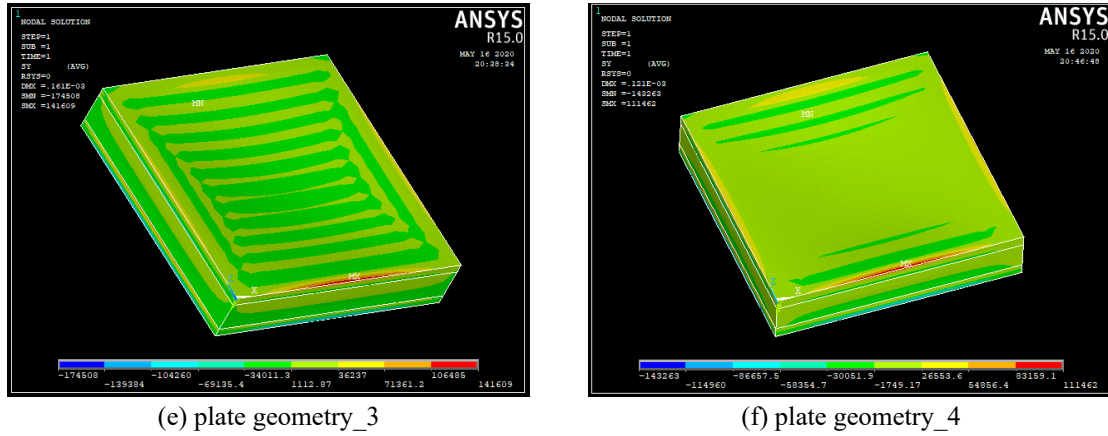


Fig. 7 Continued

Table 7 Effect of enhancing thickness of faceplate of plate on the non-dimensionalised fundamental frequency for square sandwich plate i.e., CCCC, $R=5$

Non-dimensionalised fundamental frequency (ω)	Mode No.	Ratio of thickness of the face plate to depth of the plate (T/h)					
		0.00	0.08	0.10	0.14	0.18	0.22
	M_1	0.6699	10.7520	11.3761	13.1115	15.3509	18.0510
	M_2	1.0925	17.6250	18.4668	20.6508	23.2969	26.4570
	M_3	1.1854	17.7028	19.4128	24.3912	30.5433	37.4137
	M_4	1.2396	23.0020	24.6860	29.6550	33.9870	38.3379
	M_5	1.2772	26.3644	27.3416	30.3562	35.8374	42.8703
	M_6	1.5173	26.6990	30.3959	36.3175	41.3129	46.1344
	M_7	1.526	29.0124	31.2691	37.4175	44.0705	51.7460
	M_8	1.6338	30.3789	32.0724	39.9407	46.3253	52.5606
	M_9	1.6858	30.8042	34.2592	41.1503	48.5688	55.3976
	M_{10}	1.9376	35.6975	36.9506	42.3146	49.4609	56.3067

been employed. The analysis has been done for different geometry of the plate represented in table 7. From the Table 7, we can observe that non-dimensionalised fundamental frequency improves with enhancing thickness of faceplate if plate depth remains unity.

4.5 Harmonic analysis

Harmonic response is demonstrated to obtain resonance amplitude at its natural frequency. These parameters are presented on the graph known as function response function (FRF). In this paper, square plate with sandwich structure has been studied to observe the result of increasing thickness ratio on natural frequency and resonance amplitude. The damping ratio has been taken as 0.01. The results are tabulated in Table 8 including the phase change angle. We can observe from Table 8 that natural frequency (NF) increases with improving the thickness proportion and resonance amplitude (RA) decreases for the same case. If a very thin faceplate of $0.8h$ thickness was built with same plate the percentage reduction improves by 33.83%.

Harmonic behaviors of the sandwich plates have been offered for FRF shown in Fig. 8 (a)-(f).

Table 8 Effects of increasing thickness ratio (T_f/h) (taking $R=5$, damping factor=0.01 and Clamped BC)

G. No	T_f/h	N.F. (Hz)	R.A. (m)	Phase change Angle	% decrement in R.A.
1	0	31.989	0.0949765	-88.1398°	0.00
2	0.08	56.883	0.0628400	-85.4113°	33.83
3	0.10	60.189	0.0573575	-90.1787°	39.61
4	0.14	69.370	0.0223645	-89.934°	76.45
5	0.18	81.219	0.0168606	-90.261°	82.25
6	0.22	95.500	0.0125984	-89.5077°	86.74

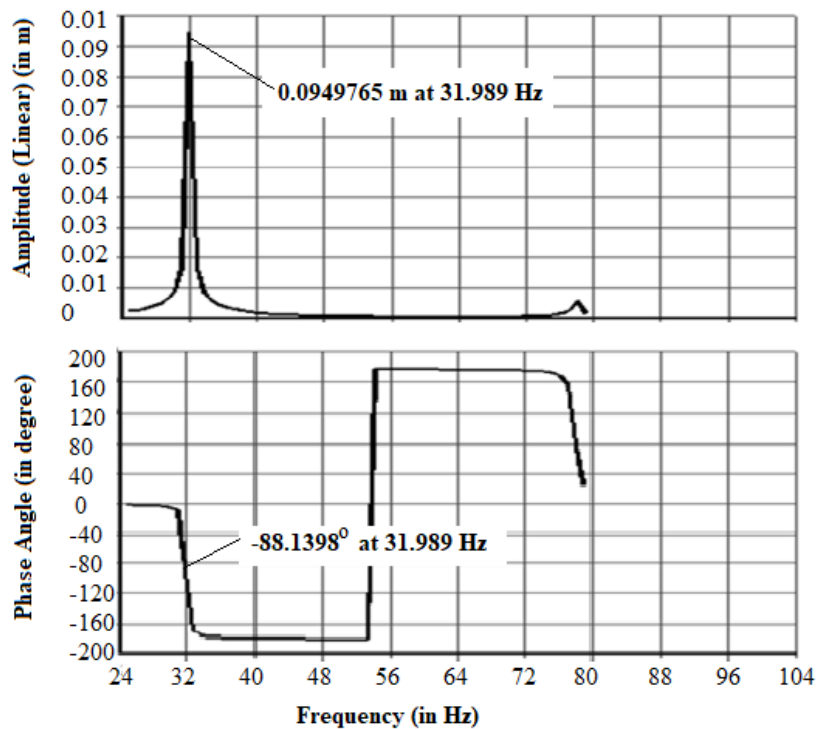


Fig. 8(a) FRF for Isotropic plate

Graphs of Fig. 8 present relation of frequencies verses amplitude and phase angle. Maximum value of the amplitude, called resonance, occurred at its natural frequency.

FRF (for geometry 1) is shown in Fig. 8(a). From figure, it can be seen that resonant amplitude “0.0949765 m” has been found at its natural frequency of 31.989 Hz and the amplitude changes its phase at an angle “-88.1398°”.

Resonant amplitude “0.0619540 m” appeared at natural frequency of 56.883 Hz for geometry 2 as shown in Fig. 8(b) and phase change angle “-85.4113°” found for resonant amplitude.

Fig. 8(c) shows FRF for geometry 3. Resonant amplitude “0.0619540 m” and Phase change angle “-90.1787°” occurred at natural frequency of 60.189 Hz.

For geometry 4, Resonant amplitude “0.0223645 m” and Phase change angle “-89.934°” found at natural frequency of 69.37 Hz as shown in figure 8(d).

Resonant amplitude “0.0168606 m” and Phase change angle “-90.261°” found at natural

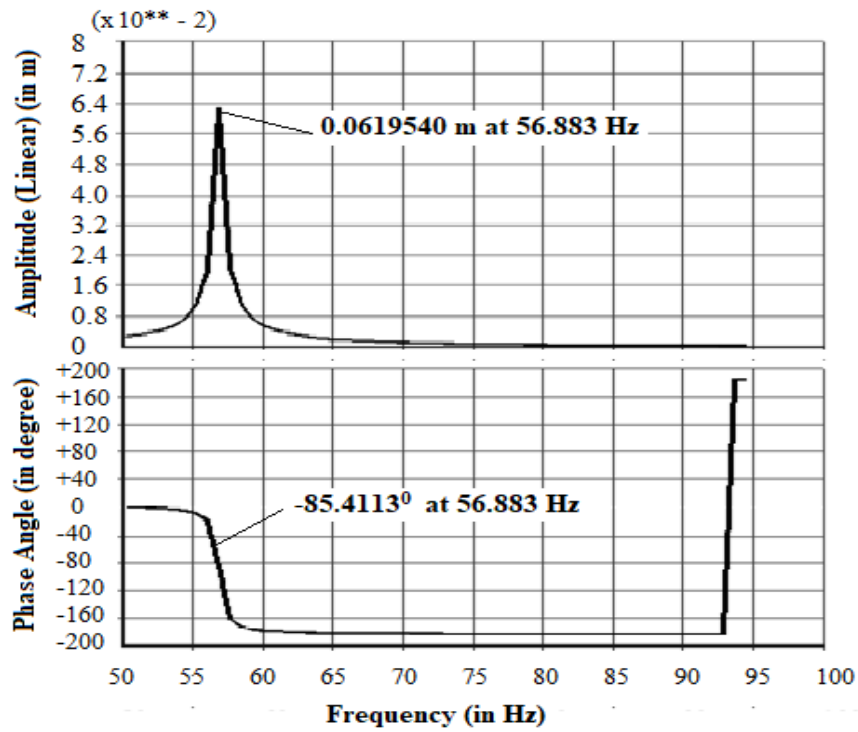


Fig. 8(b) FRF for thickness ratio (T_f/h) as 0.08

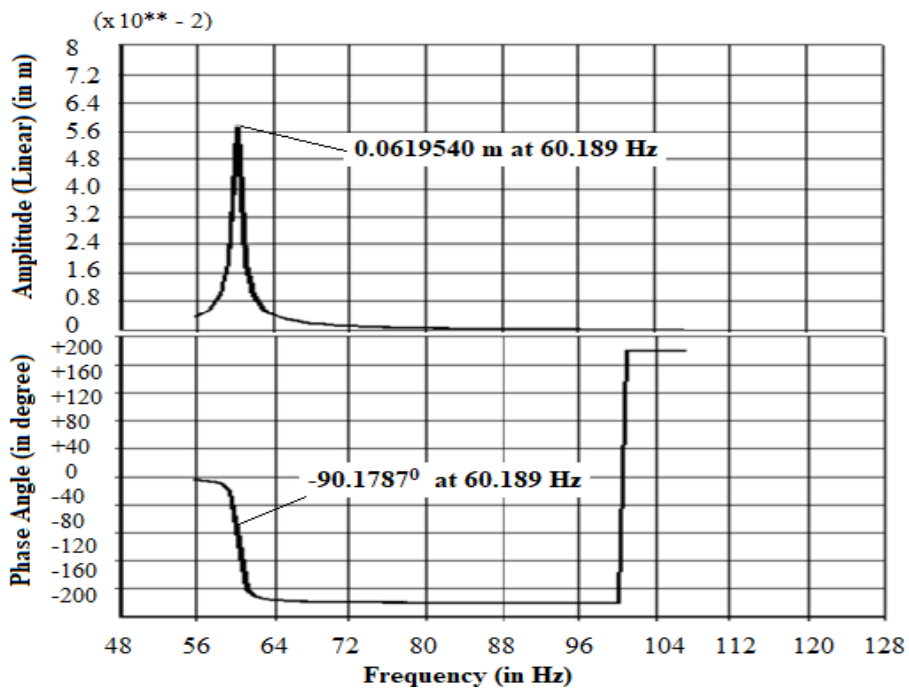


Fig. 8(c) FRF for thickness ratio (T_f/h) as 0.10

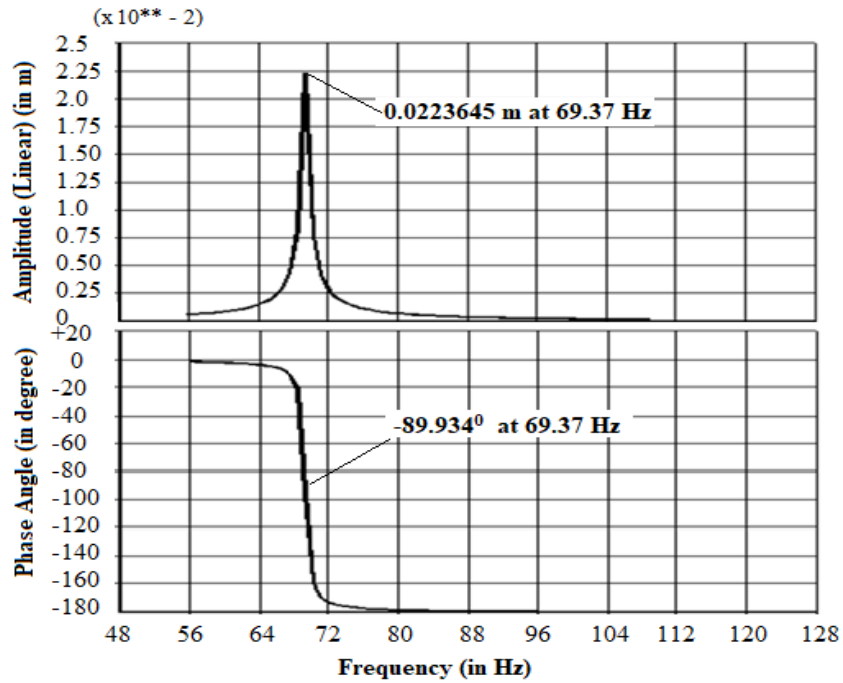


Fig. 8(d) FRF for thickness ratio (T_f/h) as 0.14

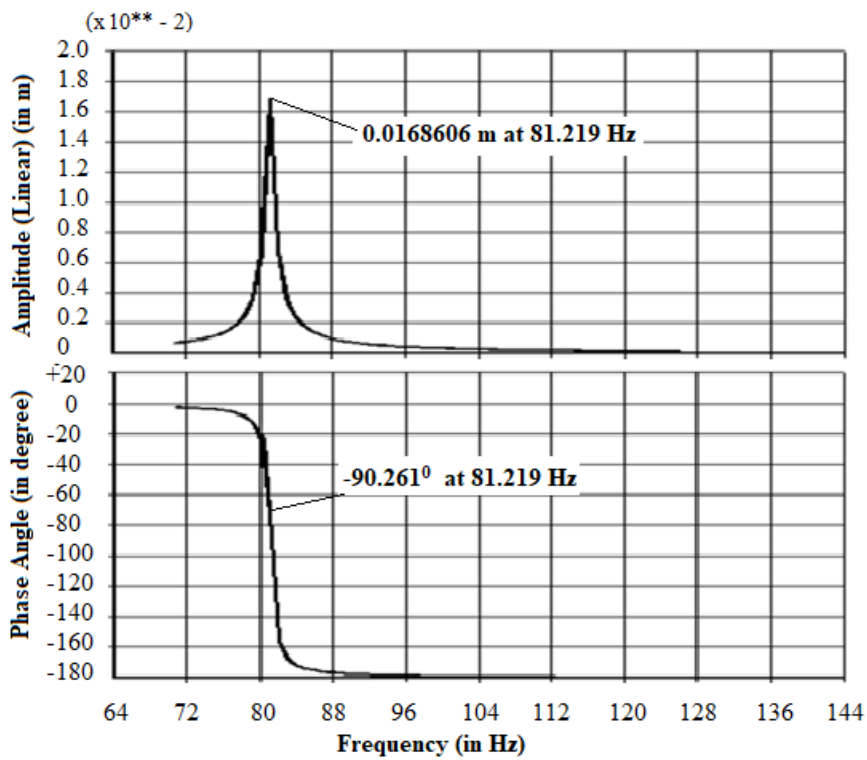


Fig. 8(e) FRF for thickness ratio (T_f/h) as 0.18

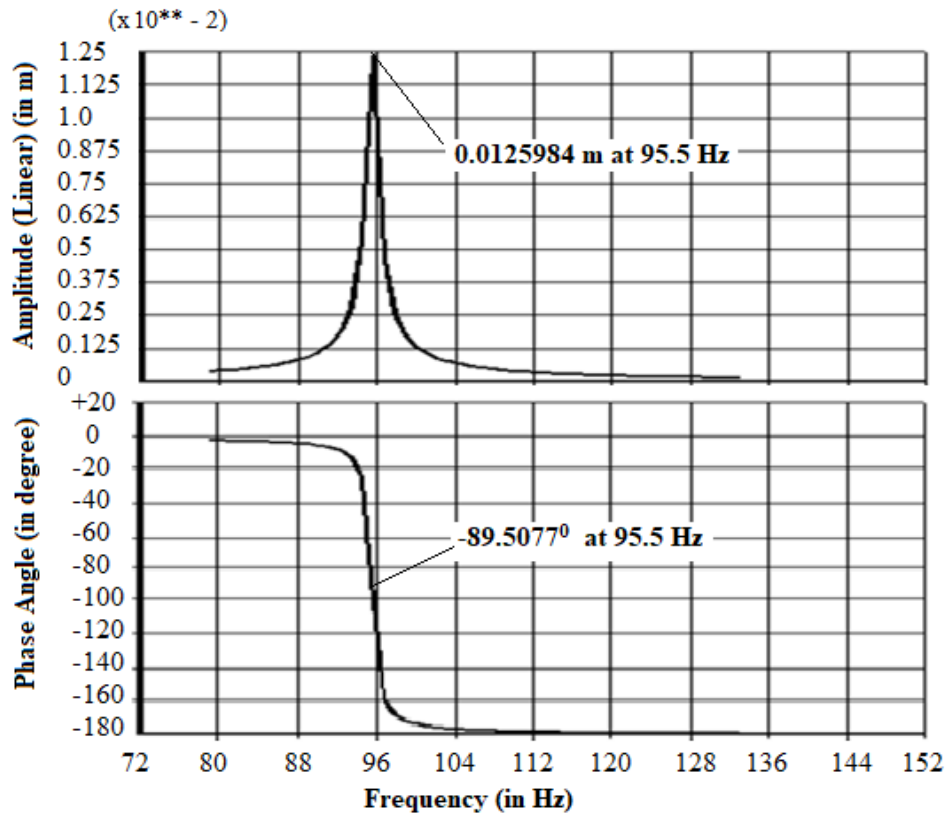


Fig. 8(f) FRF for thickness ratio (T/h) as 0.22

frequency of 81.219 Hz for geometry 5 as shown in Fig. 8(e).

Resonant amplitude “0.0125984 m” and Phase change angle “-89.5077°” occurred at natural frequency of 95.5 Hz for geometry 6 as shown in Fig. 8(f).

5. Conclusions

The main objective of this research is to design a light weight plate which resists vibration. Static, vibration and harmonic behaviour of the sandwich plates are studied in this paper to fulfil the objective.

Various geometries of the square sandwich plate containing various thicknesses of face sheet were created. The convergence behaviour is verified and found that a (24×24) meshing size is good enough to obtain the results. Additionally, outcomes were validated by relating with published work in open domain and were in excellent agreement. Effects of increasing thickness proportion on frequency and maximum amplitude was listed. After study, following were the main outcomes:

- The reduction in the weight is achieved while increasing the thickness ratio.
- The stress and resonance amplitude of isotropic plate found high but non-dimensionalized fundamental frequency found low as compared to the sandwich plate.

- The increment of percentage reduction for both stress and maximum amplitude observed if thickness ratio is increased.
- The stress is reduced by 74.35% and percentage decrease of maximum amplitude is improved through 33.83% by using a very thin faceplate of 0.08h thickness as cover plate in same sheet.
- It is also observed that sheet having thick cover plate produces minimum vibration and possesses minimum weight.

References

- Abdennadher, M., Wali, M., Fakhfakh, T. and Haddar, M. (2009), "Dynamic analysis of sandwich structure in presence of shock", *Mach. Dyn. Prob.*, **33**(2), 5-18.
- Abo Sabah, S.H. and Kueh, A.B.H. (2014), "Finite element modeling of laminated composite plates with locally delaminated interface subjected to impact loading", *Scientif. World J.*, **2014**, Article ID 954070. <http://doi.org/10.1155/2014/954070>.
- Al-Fasih, M.Y., Kueh, A.B.H. and Ibrahim, M.H.W. (2020), "Failure behavior of sandwich honeycomb composite beam containing crack at the skin", *Plos One*, **15**(2), 1-19. <https://doi.org/10.1371/journal.pone.0227895>.
- Belarbi, M.O., Tati, A., Ounis, H. and Khechai, A. (2017), "On the free vibration analysis of laminated composite and sandwich plates: A layerwise finite element formulation", *Lat. Am. J. Solid. Struct.*, **14**, 2265-2290. <https://doi.org/10.1590/1679-78253222>.
- Caprino, G., Lopresto, V., Scarponi, C. and Briotti, G. (1999), "Influence of material thickness on the response of carbon-fabric/epoxy panels to low velocity impact", *Compos. Sci. Technol.*, **59**, 2279-2286. [https://doi.org/10.1016/S0266-3538\(99\)00079-2](https://doi.org/10.1016/S0266-3538(99)00079-2).
- Gopichand, A., Krishnaiah, G., Krishna, M., Reddy, V.D. and Sharma, A.V.N.L. (2012), "Design and analysis of corrugated steel sandwich structures using ANSYS workbench", *Int. J. Eng. Res. Technol.*, **1**(8), 1-8.
- Hanna, N.F. and Leissa, A.W. (1994), "A higher order shear deformation theory for the vibration of thick plates", *J. Sound Vib.*, **170**(4), 545-555. <https://doi.org/10.1006/jsvi.1994.1083>.
- Icardi, U. and Ferrero, L. (2009), "Impact analysis of sandwich composites based on a refined plate element with strain energy updating", *Compos. Struct.*, **89**, 35-51. <https://doi.org/10.1016/j.compstruct.2008.06.018>.
- Krzyzak, A., Mazur, M., Gajewski, M., Drozd, K., Komorek, A. and Przybylek, P. (2016), "Sandwich structured composites for aeronautics: methods of manufacturing affecting some mechanical properties", *Int. J. Aerosp. Eng.*, **4**, 1-10. <https://doi.org/10.1155/2016/7816912>.
- Kulkarni, S.D and Kapuria, S. (2008), "Free vibration analysis of composite and sandwich plates using an improved discrete kirchhoff quadrilateral element based on third-order zigzag theory", *Comput. Mech.*, **42**, 803-824. <https://doi.org/10.1007/s00466-008-0285-z>.
- Lashin, M.M. and El-Nady, A.O. (2015), "Free vibration analysis of sandwich beam structure using finite element approach", *IOSR J. Mech. Civil Eng.*, **12**(6), 34-42. <http://doi.org/9790/1684-12613442>.
- Li, X., Li, G. and Wang, C.H. (2011), "Optimisation of composite sandwich structures subjected to combined torsion and bending stiffness requirements", *Appl. Compos. Mater.*, **19**, 689-704. <https://doi.org/10.1007/s10443-011-9221-z>.
- Malekzadeh, K. and Sayyidmousavi, A. (2009), "Free vibration analysis of sandwich plates with a uniformly distributed attached mass, flexible core, and different boundary conditions", *J. Sandw. Struct. Mater.*, **12**, 709-732. <https://doi.org/10.1177/1099636209343383>.
- Meunier, M. and Sheno, R.A. (1999), "Free vibration analysis of composite sandwich plates", *Proc. Inst. Mech. Eng.*, **213**, 715-727.
- Mondal, S., Patra, A.K., Chakraborty, S. and Mitra, N. (2015), "Dynamic performance of sandwich composite plates with circular hole/cut-out: A mixed experimental-numerical study", *Compos. Struct.*,

- 131**, 479-489. <https://doi.org/10.1016/j.compstruct.2015.05.046>.
- Pagani, A., Valvano, S. and Carrera, E. (2018), "Analysis of laminated composites and sandwich structures by variable-kinematic MITC9 plate elements", *J. Sandw. Struct. Mater.*, **20**(1), 4-41. <https://doi.org/10.1177/1099636216650988>.
- Reddy, J.N. (1997). *Mechanics of Laminated Composite Plates and Shells: Theory and Analysis*, CRC Press Boca Raton, New York.
- Rezaiee-Pajand, M., Arabi, E. and Masoodi, A.R. (2019), "Nonlinear analysis of FG-sandwich plates and shells", *Aerosp. Sci. Technol.*, **87**, 178-189. <https://doi.org/10.1016/j.ast.2019.02.017>.
- Rezaiee-Pajand, M., Masoodi, A.R. and Arabi, E. (2018), "On the shell thickness-stretching effects using seven-parameter triangular element", *Eur. J. Comput. Mech.*, **27**(2), 163-185. <https://doi.org/10.1080/17797179.2018.1484208>.
- Rezaiee-Pajand, M., Masoodi, A.R. and Mokhtari, M. (2018), "Static analysis of functionally graded non-prismatic sandwich beams", *Adv. Comput. Des.*, **3**(2), 165-190. <https://doi.org/https://doi.org/10.12989/acd.2018.3.2.165>.
- Rezaiee-Pajand, M., Masoodi, A.R. and Rajabzadeh-Safaei, N. (2019), "Nonlinear vibration analysis of carbon nanotube reinforced composite plane structures", *Steel Compos. Struct.*, **30**(6), 493-516. <https://doi.org/10.12989/scs.2019.30.6.493>.
- Rezaiee-Pajand, M., Mokhtari, M. and Masoodi, A.R. (2018), "Stability and free vibration analysis of tapered sandwich columns with functionally graded core and flexible connections", *CEAS Aeronaut. J.*, **9**(4), 629-648. <https://doi.org/10.1007/s13272-018-0311-6>.
- Shariyat, M. (2010), "A generalized global-local high-order theory for bending and vibration analyses of sandwich plates subjected to thermo-mechanical loads", *Int. J. Mech. Sci.*, **52**, 495-514. <https://doi.org/10.1016/j.ijmecsci.2009.11.010>.
- Soufeiani, L., Ghadyani, G., Kueh, A.B.H. and Nguyena, K.T.Q. (2017), "The effect of laminate stacking sequence and fiber orientation on the dynamic response of FRP composite slabs", *J. Build. Eng.*, **13**, 41-52. <https://doi.org/10.1016/j.job.2017.07.004>.
- Wang, C.M., Ang, K.K. and Yang, L. (2000), "Free vibration of skew sandwich plates with laminated facings", *J. Sound Vib.*, **235**(2), 317-340. <https://doi.org/10.1006/jsvi.2000.2918>.